THE ASTROPHYSICAL JOURNAL, 615:L61–L64, 2004 November 1

DIFFERENTIAL IMAGING WITH A MULTICOLOR DETECTOR ASSEMBLY: A NEW EXOPLANET FINDER CONCEPT

CHRISTIAN MAROIS,[1] RENÉ RACINE,[1] RENÉ DOYON,[1] DAVID LAFRENIÈRE,[1] AND DANIEL NADEAU[1]
Observatoire du Mont Mégantic and Département de Physique, Université de Montréal, Montréal, QC H3C 3J7, Canada; marois@astro.umontreal.ca, racine@astro.umontreal.ca, doyon@astro.umontreal.ca, david@astro.umontreal.ca, nadeau@astro.umontreal.ca
Received 2003 June 27; accepted 2004 September 23; published 2004 October 4

ABSTRACT

Simultaneous spectral differential imaging is a high-contrast technique by which subtraction of simultaneous images reduces noise from atmospheric speckles and optical aberrations. Small non–common-wave-front errors between channels can seriously degrade its performance. We present a new concept, a multicolor detector assembly, which can eliminate this problem. The device consists of an infrared detector and a microlens array onto the flat side of which a checkerboard pattern of narrowband microfilters is deposited, each microfilter coinciding with a microlens. Practical considerations for successful implementation of the technique are mentioned. Numerical simulations predict a noise attenuation of 10^{-3} at 0.″5 for a 10^5 s integration on a $m_H = 5$ star of Strehl ratio 0.9 taken with an 8 m telescope. This reaches a contrast of 10^{-7} at an angular distance of 0.″5 from the center of the star image.

Subject headings: instrumentation: adaptive optics — instrumentation: detectors — planetary systems — stars: imaging

Online material: color figure

1. INTRODUCTION AND MOTIVATION

Direct imaging and spectroscopy of exoplanets are crucial to constrain their masses, study their atmospheres, and ultimately find telltale signatures of life. The task is dauntingly difficult. The planet image is hugely fainter than the background from the brilliant stellar image. The most obvious problem is photon noise in the bright star point-spread function (PSF). A remedy is coronagraphy (Lyot & Marshall 1933; Roddier & Roddier 1997; Rouan et al. 2000; Baudoz et al. 2000; Abe et al. 2001; Kasdin et al. 2003), which attenuates the coherent diffraction pattern of the on-axis PSF. At high Strehl ratios the diffraction pattern dominates much of the PSF and coronagraphs can achieve strong attenuation (Kilston et al. 2002). With the relatively modest Strehl ratios achieved with current adaptive optics (AO) systems on large ground-based telescopes, the efficiency of coronagraphy is limited by the presence of a rapidly changing halo of speckles generated by atmospheric phase distortion. This increases the local PSF variance by orders of magnitude above that caused by photon noise (Racine et al. 1999). In addition, aberrations in the optical train, unfiltered by the AO system, produce speckles of a much longer lifetime, hence much brighter in a long-exposure image, than atmospheric speckles. This noise can be dominant for integrations longer than a few seconds (Marois et al. 2003a, 2004). Quasi-static speckles also limit the high-contrast performance of the *Hubble Space Telescope* (*HST*; Schneider & Silverstone 2003) in the form of the so-called breathing problem. All this underscores the importance of PSF calibration for high-contrast imaging, which is the topic of this Letter.

Simultaneous spectral differential imaging (Smith 1987; Racine et al. 1999; Marois et al. 2000a; Sparks & Ford 2002; Biller et al. 2004) is such a calibration technique. Images are acquired simultaneously at adjacent wavelengths in a spectral range where the planetary and stellar spectra differ appreciably. Judicious image subtraction removes the stellar image and conserves that of any companion. A useful spectral feature for this purpose is the sharp methane absorption band head at 1.6 μm (Rosenthal et al. 1996) found in relatively cold atmospheres (Burgasser et al. 2002) such as those of cold T-type brown dwarfs and Jovian planets.

The TRIDENT camera (Marois et al. 2000b, 2003a, 2003b, 2003c, 2004), a three-channel (1.580, 1.625, and 1.680 μm, 1% bandwidth) differential imager, has been extensively used with the AO system of the 3.6 m Canada-France-Hawaii Telescope (Rigaut et al. 1998). From the data, one can determine the level of noise attenuation achieved. The noise attenuation factor $\Delta N/N$ is defined as the median over an annulus of the pixel-by-pixel ratio of the absolute value of the intensity in the difference image to its absolute value in the original image after subtraction of an azimuthally averaged profile. The noise structure of the PSF at one wavelength is dominated by static aberrations and is well approximated with ~130 nm of static phase screen following a power-law distribution $P \propto \nu^{\alpha}$ with $\alpha = -2.7$. This level of aberration is consistent with that measured (110 nm rms) for the static component of the Probing the Universe with Enhanced Optics AO system (Rigaut et al. 1998). Figure 1 illustrates typical noise attenuations obtained with TRIDENT. At subarcsecond separations the noise residuals in a difference image are ~10 times larger than the sum of the photon and read noises. Results from numerical simulations indicate that ~$\lambda/20$ of non–common-path aberrations can explain TRIDENT limited performance. A factor of ~4 improvement is obtained by subtraction of the residuals of a reference star observed shortly after and under the same conditions as the science target. This indicates that differential aberrations between channels contribute a large fraction of the residual noise in a difference of simultaneous images. It also appears that some of the noise after subtraction of the reference star image is caused by slight changes in optical aberrations between the target and the reference star observations.

In this Letter, in light of the non–common-path limitations, a new differential imager concept is introduced that should improve detection limits by a large factor. Simulations are made to estimate the performances and the expected detection limits with 8 m class telescopes and high-order AO systems.

[1] Visiting Astronomer, Canada-France-Hawaii Telescope, operated by the National Research Council of Canada, the Centre National de la Recherche Scientifique, France, and the University of Hawaii.

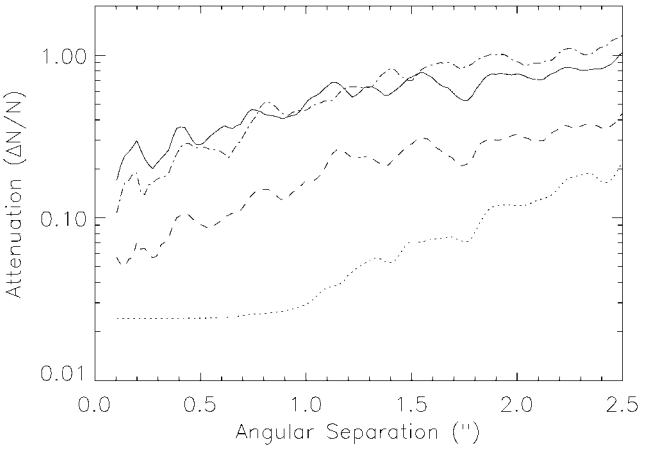

FIG. 1.—Median of the pixel-by-pixel ratio of residual noise to initial noise as a function of the distance from the PSF center for (1) the difference of two simultaneous TRIDENT images (*solid line*), (2) the difference between differences of simultaneous TRIDENT images of two stars observed sequentially (*dashed line*), (3) a difference image whose noise would only consist of the speckle, read, photon, and flat-field noises of the TRIDENT images (*dotted line*), and (4) a simulated difference image with the same noises plus an rms wave-front difference between channels of λ/20 (*dot-dashed line*).

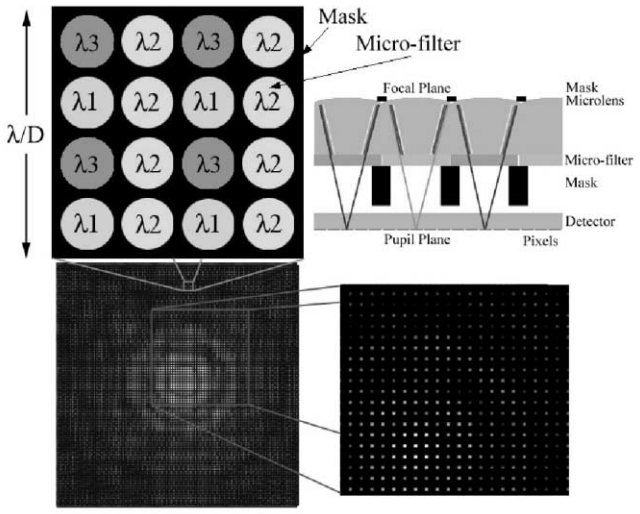

FIG. 2.—Concept of a three-wavelength differential imager with an MCDA showing the whole assembly (*top right*) and the microfilter array (*top left*). Here, each microlens covers a 5 × 5 pixel cluster. A PSF and one of its checkerboard monochromatic samples are shown at the bottom. See text for details. [*See the electronic edition of the Journal for a color version of this figure.*]

2. THE MULTICOLOR DETECTOR ASSEMBLY CONCEPT

A solution to the non–common-path problem is to perform the spectral separation in the image plane of a single optical path imager with a Multicolor Detector Assembly (MCDA). A three-wavelength MCDA is illustrated in Figure 2. A microlens array located at the focal plane is used to concentrate the light of each PSF spatial sample into well-separated detector pixels (each microlens covers a 5 × 5 pixel cluster) in order to minimize interpixel crosstalk, as discussed below. A mask on both faces of the microlens array blocks the light that may scatter between microlenses. Each microlens in a 2 × 2 microlens cluster is covered with one of three different microfilters, two microlenses having the same filter for signal-to-noise ratio optimization. The fact that only a small central area of each microfilter is used relaxes the requirement for edge-to-edge filter uniformity. A detector readout yields four critically sampled "checkerboard" images of the PSF, one at each wavelength, that can be interpolated to construct a filled image.

The attenuation of noise structures allowed by this device, in the absence of photon, read, and flat-field noises, can theoretically be arbitrarily large if the noise structures—speckles—are critically sampled at each wavelength over a PSF image whose extent is unlimited. This is so because by the sampling theorem for bandwidth-limited images, it is then possible to perfectly interpolate the pixel intensity at a given wavelength for any pixel that is "blind" at that wavelength. Complete attenuation is of course not achievable in practice because the idealized conditions posed above cannot be realized. Flat-field errors will probably be the dominant limitation at high flux levels. The MCDA itself may entail limiting factors such as the two mentioned below.

The microlens array is required to minimize signal cross talk between PSF sampling points. With current infrared detectors, a pixel can leak as much as 40% of its signal to its adjacent pixels (Finger et al. 1998). Diffraction by the microlenses can also be a significant source of cross talk. Cross talk limits the PSF noise attenuation as follows. The distance of a speckle to the PSF center is proportional to wavelength. PSFs obtained at different wavelengths must be rescaled before being subtracted. The leak of a speckle signal sampled at one wavelength to a sampling point for another wavelength no longer coincides spatially with itself after rescaling. Subtraction of the rescaled images leaves a residual whose intensity is equal to the cross talk coefficient X times the difference in the speckle intensity between the radially shifted samples. The average residual noise after image subtraction then increases from zero at the PSF center, where the wavelength shift is nil, to X times its initial level when the radial shift between wavelengths exceeds the FWHM ($\sim\lambda/D$) of the speckles, i.e., at an angular offset $\theta > \lambda^2/(\Delta\lambda D)$. At larger offsets, the cross talk–induced noise saturates at an amplitude of X times the speckle intensity and the limiting attenuation factor becomes equal to the cross talk level X. Numerical simulations (Fig. 3) confirm this analysis. It is expected that sample separations $\sim 5 \times 18.5$ μm pixels (to reduce charge leaks between samples to less than 0.001) and microlens f-ratios less than 17 (to limit the spillover of a pupil

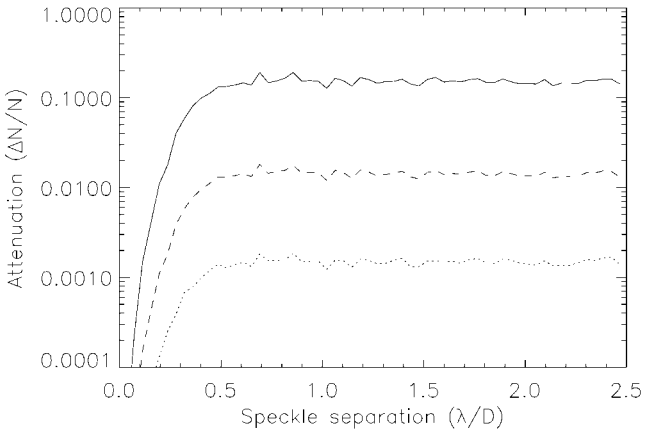

FIG. 3.—Effect of sample-to-sample cross talk in an MCDA from numerical simulations. This shows the noise attenuation achieved by the subtraction of two PSF samples as a function of speckle separation with wavelength, expressed in λ/D units, when attenuation is only limited by 0.001 (*dotted line*), 0.01 (*dashed line*), and 0.1 (*solid line*) of the sample-to-sample cross talk.

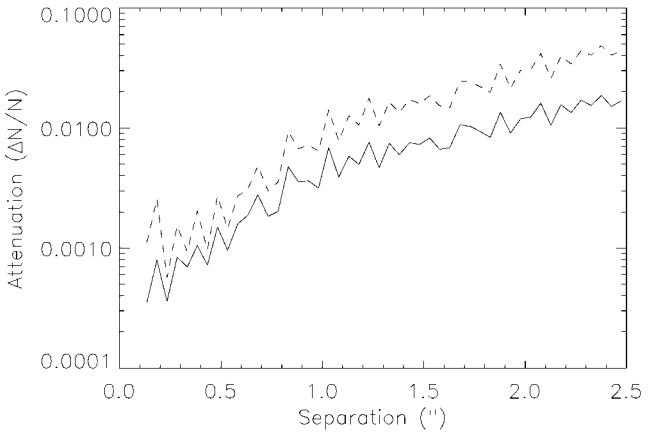

FIG. 4.—PSF noise attenuation around an $m_H = 5$ star observed for 10^5 s with an 8 m telescope, a high-order AO system delivering a Strehl ratio of 0.91, a three-wavelength MCDA, and 20% global optical transmission without (*solid line*) and with (*dashed line*) a Lyot coronagraph. The latter features a Gaussian mask with a FWHM of 15 λ/D and a 60% transmissive Lyot mask.

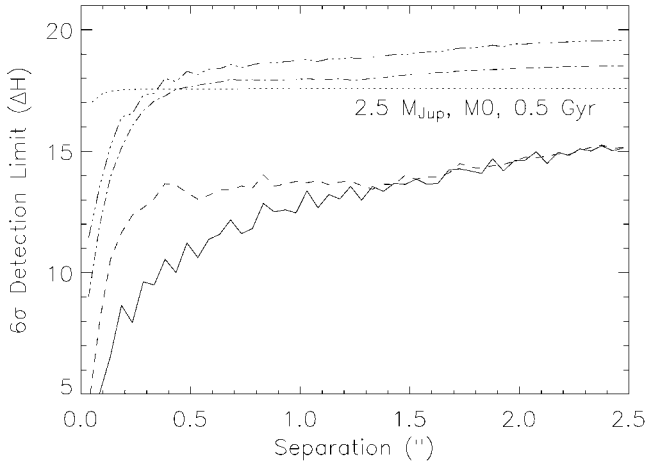

FIG. 5.—6 σ detection limit with (*triple-dot–dashed line*) and without (*dot-dashed line*) a Lyot coronagraph after multicolor speckle suppression. The dashed and solid lines show, respectively, the noise of a single PSF with and without a Lyot coronagraph. The dotted line shows the magnitude difference for a 0.5 Gyr/2.5$M_{\rm Jup}$ (from Baraffe et al. 2003) companion around a M0 star at 10 pc, including the effect of stellar flux reflection by the companion at small separations.

diffraction pattern onto an adjacent pupil image) will allow $X < 0.001$ at $\lambda \sim 1.6$ μm.[2] To minimize the sample-to-sample cross talk and to block gaps between microlenses, two masks are introduced above and under the microlens array.

PSF decorrelation between wavelengths can also occur with an MCDA if the optical path is chromatic. Refractive optics produce wave fronts of different dimensions at different wavelengths because of the wavelength dependence of the index of refraction. Atmospheric dispersion also decorrelates the PSFs' noise structure because the wave fronts for different wavelengths follow different optical paths through the atmosphere and instrument. This leads to non–common-path errors since the footprints on optical surfaces of wave fronts at different wavelengths will be sheared. Simulations indicate that a ~1/1000 wave-front shear limits attenuation to $\sim 10^{-3}$. The effects of chromatism and atmospheric refraction can be mitigated by using reflective optics and atmospheric dispersion compensators.

3. SIMULATED PERFORMANCE WITH AN MCDA

Numerical simulations were done to estimate the PSF noise attenuation achievable with a three-wavelength ($\lambda_1 = 1.52$ μm, $\lambda_2 = 1.58$ μm, and $\lambda_3 = 1.64$ μm) MCDA in quasi-realistic conditions. Simulations are for a 10^5 s total integration divided in 60 s exposures on an $m_H = 5$ star observed with an 8 m telescope and 4*k* actuator AO system of 20% transmission and 2% bandpass. AO phase filtering is simulated by choosing a flat power spectrum for spatial frequencies lower than twice the interactuator spacing. Static aberrations are included using a power-law power spectrum with $\alpha = -2.7$ to obtain 100 nm rms total aberrations, of which 15 nm rms are not corrected by the AO system because of non–common-path optics. The three images are the average of 500 atmospheric speckle realizations for 0.″5 seeing at 0.5 μm. AO filtering of both the static and the Kolmogorov atmospheric phase screens yields PSFs with Strehl ratios of 0.96 at 1.60 μm. These also include a typical level of read noise of 5 e^- pixel^{-1} per 60 s exposure, photon noise, random flat-field errors of 10^{-4}, sky noise, and sample-to-sample cross talk of 10^{-3}. PSF evolution with wavelength is included and partly compensated by an appropriate combination of the multiwavelength images (Marois et al. 2000a; Marois 2004). For the sake of completeness, simulations were done both with and without an optimized Lyot coronagraph. For the coronagraph simulation, the 15 nm rms unfiltered static aberrations are split in two uncorrelated 10 nm rms aberrations that are, respectively, included before and after the coronagraph. The results are shown in Figure 4. These lead to the detection limits (Fig. 5), checked with off-axis companion images, which are compared to the contrast required for the detection of 2.5$M_{\rm Jup}$ exoplanets around 0.5 Gyr M0 stars (Baraffe et al. 2003). When combined with an MCDA, the coronagraph does ~1 mag better. The coronagraph has effectively attenuated the PSF structure by an order of magnitude inside a 0.″5 radius, thus reducing the flat-field accuracy needed to achieve $\Delta H = 17.5$.

[2] For a circular aperture, the mean intensity diffracted at radius r is $\sim 0.04[r/(\lambda f/D)]^{-3}$ for unit central intensity. For diffraction cross talk to be less than 0.001 at a wavelength of 1.6 μm and at a distance of 5 × 18.5 μm requires $f/D < 17$.

4. SUMMARY AND CONCLUSION

Experience with the TRIDENT camera has shown that small non–common-path aberrations in multiple optical channel instruments seriously limit PSF noise attenuation and, hence, faint companion detection. The MCDA concept described here can overcome this problem. Numerical simulations predict that with an MCDA, 2.5$M_{\rm Jup}$ exoplanets around 0.5 Gyr M0 stars should be detectable in 10^5 s with an 8 m telescope and a 4*k* actuator AO system.

Planet finders based on MCDAs would enable detection and characterization of exoplanets with present large telescopes and high-order AO systems. The technique is relatively simple to implement and would complement coronagraph projects, or telescopes such as *HST*, where it could calibrate evolving noise structure. An MCDA combined with a coronagraph would be a powerful tool for detecting ozone in the mid-IR (Des Marais et al. 2002), water in the near-IR, molecular oxygen in the red, and, eventually, the chlorophyll "red edge" with the Terrestrial Planet Finder. An optimized MCDA-type polarimeter could study reflected star light from exoplanets (Saar & Seager 2003)

or disks and zodiacal dust. Instead of microfilters, micropolarizers would be used to produce simultaneous polarized images with a single optical channel.

This work was supported in part through grants from NSERC, Canada, and from FQRNT, Québec.

REFERENCES

Abe, L., Vakili, F., & Boccaletti, A. 2001, A&A, 374, 1161
Baraffe, I., Chabrier, G., Barman, T. S., Allard, F., & Hauschildt, P. H. 2003, A&A, 402, 701
Baudoz, P., Rabbia, Y., & Gay, J. 2000, A&AS, 141, 319
Biller, B. A., Close, L., Lenzen, R., Brandner, W., McCarthy, D., Nielsen, E., & Hartung, M. 2004, Proc. SPIE, in press
Burgasser, A. J., et al. 2002, ApJ, 564, 421
Des Marais, D. J., et al. 2002, Astrobiology, 2, 153
Finger, G., Biereichel, P., Mehrgan, H., Meyer, M., Moorwood, A. F. M., Nicolini, G., & Stegmeier, J. 1998, Proc. SPIE, 3354, 87
Kasdin, N. J., Vanderbei, R. J., Spergel, D. N., & Littman, M. G. 2003, ApJ, 582, 1147
Kilston, S., et al. 2002, Terrestrial Planet Finder Architecture Study, Final Report (Boulder: Ball Aerospace)
Lyot, B., & Marshall, R. K. 1933, JRASC, 27, 225
Marois, C. 2004, Ph.D. thesis, Univ. Montréal
Marois, C., Doyon, R., Racine, R., & Nadeau, D. 2000a, PASP, 112, 91
———. 2000b, Proc. SPIE, 4008, 788
———. 2003a, in EAS Pub. Ser. 8, Astronomy with High Contrast Imaging: From Planetary Systems to Active Galactic Nuclei, ed. C. Aime & R. Soummer (Nice: EDP), 233
Marois, C., Doyon, R., Racine, R., Nadeau, D., Riopel, M., Vallée, P., & Lafrenière, D. 2004, PASP, submitted
Marois, C., Nadeau, D., Doyon, R., & Racine, R. 2003b, Proc. SPIE, 4860, 130
———. 2003c, in IAU Symp. 211, Brown Dwarfs, ed. E. L. Martín (San Francisco: ASP), 275
Racine, R., Walker, G. A. H., Nadeau, D., Doyon, R., & Marois, C. 1999, PASP, 111, 587
Rigaut, F., et al. 1998, PASP, 110, 152
Roddier, F., & Roddier, C. 1997, PASP, 109, 815
Rosenthal, E. D., Gurwell, M. A., & Ho, P. T. P. 1996, Nature, 384, 243
Rouan, D., Riaud, P., Boccaletti, A., Clénet, Y., & Labeyrie, A. 2000, PASP, 112, 1479
Saar, S. H., & Seager, S. 2003, in ASP Conf. Ser. 294, Scientific Frontiers in Research on Extrasolar Planets, ed. D. Deming & S. Seager (San Francisco: ASP), 529
Schneider, G., & Silverstone, M. D. 2003, Proc. SPIE, 4860, 1
Smith, W. H. 1987, PASP, 99, 1344
Sparks, W. B., & Ford, H. C. 2002, ApJ, 578, 543